sciendo

POLISH MARITIME RESEARCH 2 (118) 2023 Vol. 30; pp. 28-38
10.2478/pomr-2023-0019

DYNAMIC POSITIONING CAPABILITY ASSESSMENT BASED ON OPTIMAL THRUST ALLOCATION

Agnieszka Piekło
Maritime Advanced Research Centre, Poland
Anna Witkowska
Poland
Tomasz Zubowicz*
Gdańsk Uniwersity of Technology, Poland

* Corresponding author: *tomasz.zubowicz@pg.edu.pl (Tomasz Zubowicz)*

ABSTRACT

The article presents an efficient method of optimal thrust allocation over the actuators in a dynamically positioned ship, according to the DNV-ST-0111 standard, Level 1. The optimisation task is approximated to a convex problem with linear constraints and mathematically formulated as quadratic programming. The case study is being used to illustrate the use of the proposed approach in assessing the DP capability of a rescue ship. The quadratic programming-based approach applied for dynamic positioning capability assessment allows for fast calculations to qualitatively compare different ship designs. In comparison with the DNV tool, it gives 100% successful validation for a ship with azimuth thrusters and a pessimistic solution for a ship equipped with propellers with rudders. Therefore, it can be safely applied at an early design stage.

Keywords: optimal thrust allocation, dynamic positioning, quadratic programming

INTRODUCTION

Dynamic positioning (DP) is one of the ship's operational states in which its relative or absolute position and heading are automatically maintained at desired set points. This goal is achieved by using only the ship's own, active thrusters without any mooring lines or other equipment. For safety reasons, the DP propulsion system configuration is maintained over-actuated. In turn, the DP control system (DPCS) applied solves continuously the stabilising control task by utilising advanced, closed-loop, model-based algorithms with the aim of achieving high disturbance rejection capabilities to cope with the vast influence of the environmental conditions at sea.

A DP capability defines a ship's station-keeping ability under given environmental conditions. The assessment of a vessel's ability to keep its position is critical for planning and executing safe and reliable DP operations. A leading classification society, Det Norske Veritas (DNV), has developed a standard for DP station-keeping capability assessments, provided in DNV-ST-0111 [1]. The standard identifies DP capability as numbers corresponding to the Beaufort scale and capability plots (in polar form). The main drawback of [1] is that it does not formulate explicitly the calculation procedures for DP assessment. Three different DP capability levels are defined, each requiring a specific assessment method. *Level 1*, considered in this paper, is specified for mono-hull ships. The calculation method at this level shall be based on a static balance of environmental and the vessel's actuator forces, assuming the same specified environmental data for all vessels. The static balance shall

determine the thrust distribution among thrusters (both magnitude and direction), called thrust allocation (TA). In some specific cases, it comes down to a simple solution of a 3-DOF problem with three unknown parameters, as implemented in [2] and [3]. However, in most cases, this task has no unique solution since the DP-capable ships are usually over-actuated. Considering thrust vector components as more than the equilibrium equations, the DP capability assessment task evolves to an optimal TA problem.

A general overview of marine control systems and an optimal TA problem are given in [4], [5]. Considering the task formulation and the approach to finding its solution, two categories of methods are identified based on the available literature. The first consists of gradient-based optimisation techniques. Here, the quadratic programming (QP) or Lagrangian multipliers-based methods are typically used [6]. Both assume that the objective function and constraints are smooth, and guarantee reaching a global minimum in a finite time. In turn, the second group of methods consists of the so-called non-gradient (derivative-free) methods. This group is represented by the meta-heuristic algorithms [7]. These include, e.g., particle swarm optimisation [8], genetic or evolutionary algorithms [9], [10], [11], [12], [13], [14], and direct-search algorithms [15]. A multi-objective optimisation-based approach to the TA problem is typically considered with application of the NSGAII algorithm [16], [17], In the latter group of algorithms, if certain requirements are met, the algorithms tends to converge to a global optimum. However, the convergence is relatively slow and there is no guarantee of reaching the solution in a finite time. In addition, different non-optimal TA strategies are also presented. These include deterministic and pseudo-inverse-based matrix methods [18], [19]. The model-based predictive control allocation [20] and adaptive control allocation [21], [22] are quite complex and, though time-consuming, allow one to take into account the actuator dynamics and uncertainties in the calculations. The subject of *optimal thrust allocation* using QP approximation is covered in [6], [23], [24], [25], [26], [27]. Related to this work, the convex optimisation approach is discussed in [8].

In this paper, the authors consider the TA problem as an optimisation task set up using the QP framework. The objective is to optimise the ship's propulsion power consumption during DP operations. The presented optimal TA method is inspired by [6]. The QP formulation is achieved by applying approximation techniques to reformulate the originally non-linear problem. With that goal, the azimuth thrusters, tunnel thruster and propeller with rudder constraints, as well as the objective function, are adopted accordingly. The proposed approach meets DNV standards and is easily adapted for the purposes of the DP capability assessment of mono-shaped ships. In this manner, the proposed solution fills the gap of the lack of calculation method details in [1]. The advantage of applying the QP-based approach is the guarantee of reaching the optimal solution in a finite time – if the solution exists. This feature is considered important for practical reasons, e.g., fast prototyping during the initial stage of a project. The structure of the underlying algorithm and the computational complexity of the calculations to be performed are also encouraging for considering the development of (online) designers' support tools. Moreover, the effect of thruster failure can also be analysed by using the DP capability plot. The presented methodology allows for a complete (all kinds of thrusters, including a propeller with the rudder) and fast in-house DP capability assessment for ship concept design. In this study, a rescue ship is used with different thruster configurations as an example. The DP capability results were compared with the existing tools offered by DNV.

The remaining section of this research work is organised in the following manner. In the *Problem Formulation* section, the DP capability assessment problem is formulated. The *Methodology* section provides information on the applied method used to propose a solution to the formulated problem. The results obtained with comparison to available external tools are discussed in the *Results* section, followed by the final *Conclusions*.

PROBLEM FORMULATION

A DP capability analysis enables one to determine the maximum environmental impact of the forces and moment that the DP system can counteract, or to design a DP actuation system that is able to withstand the prescribed disturbances. Therefore, the aim is to balance the environmental conditions by the thrust forces and moments provided by the propulsion system, which, by considering planar movement, yields:

$$\begin{aligned} \textstyle\sum_{i=1}^{N} T_{\mathrm{x}\,i} &= F_{\mathrm{env\,x}}\,, \\ \textstyle\sum_{i=1}^{N} T_{\mathrm{y}\,i} &= F_{\mathrm{env\,y}}\,, \\ \textstyle\sum_{i=1}^{N}(-T_{\mathrm{x}\,i}\cdot y_i + T_{\mathrm{y}\,i}\cdot x_i) &= M_{\mathrm{env\,z}} \end{aligned} \tag{1}$$

where $F_{\mathrm{env\,x}}$, $F_{\mathrm{env\,y}}$ and $F_{\mathrm{env\,z}}$ denote the x and y direction net force components [N] and z direction moment [Nm] resulting from the environmental influences (wind, wave and current), also considered as disturbance inputs; $T_{\mathrm{x\,i}}$ and $T_{\mathrm{y\,i}}$ indicate the x and y direction force components generated by the ith thruster [N], considered as control inputs; x_i and y_i define the position of the nth thruster in the ship-centred coordinate frame [1]; and N denotes the total number of thrusters.

Since the DPCS belongs to the class of over-actuated systems, Eq. (1) has no unique solution in terms of thruster-generated forces $T_{\mathrm{x\,i}}$ and $T_{\mathrm{y\,i}}$, $\forall i$. Therefore, instead of solving Eq. (1), the thrust is to be allocated while optimising the total power consumption (P_{total}), considering the balance equation as equality constraints. With that goal, a constrained QP formulation is applied. For the mentioned purpose, the following set of assumptions is considered.

Assumption 1. *The DP capability is achieved at the given operational conditions whenever Eq. (1) holds.*

Assumption 2. *The environmental forces in Eq. (1) are assumed to be scenario-driven, depending on the DP capability table* [1].

Assumption 3. *The relation between power and thrust can be expressed as a quadratic function with satisfactory accuracy.*

Assumption 4. *The thrust constraints imposed by the physical limits of the propulsion configuration and type can be approximated by a set of convex polygons.*

Assumptions 1 and 2 are a consequence of physical laws and do not introduce artificial limitations to the problem. From [4], it is found that the physical relationship between the produced thrust T and consumed power P can be given by the non-linear relation $P = T^{3/2}$, but it can be effectively approximated by a function of at most second degree (Assumption 3). Notably, different thruster types will have different thrust region shapes. In the general case, the constraints on the thrust form non-convex regions. By virtue of Assumptions 3 and 4, the problem is reduced to a convex one. However, this simplification can lead to a loss of precision in the power assessment.

METHODOLOGY

In the following subsection, the QP approach to thrust allocation is defined, including the propeller with rudder and thrust loss of the spoiled zone of the azimuth thruster.

DECISION VARIABLES

Considering the problem (1), a vector of decision variables is defined in the following lines.

$$\boldsymbol{u} \stackrel{\text{def}}{=} \left[T_{\text{x}\,1}, T_{\text{y}\,1}, T_{\text{x}\,2}, T_{\text{y}\,2}, \ldots, T_{\text{x}\,\text{N}}, T_{\text{y}\,\text{N}}\right]^T \quad (2)$$

The value of $\boldsymbol{u}$ is not arbitrary but is subject to constraints resulting from the propulsion type and respective location in the considered coordinate frame.

CONSTRAINTS

A direct approach to constraint formulation based on DNV-ST-0111 leads to non-linear expressions. Invoking Assumption 4, by utilising linearisation mechanisms, allows one to modify the constraints to linear form, as shown in the following lines.

Azimuth thruster

The azimuth thruster constraints arise from operational restrictions. First, flushing another operating thruster is forbidden (Fig. 1a). Second, directing the thruster to the skeg or another non-working (dead) thruster (Fig. 1a) causes a loss of thrust. The first case introduces the so-called forbidden zones, where the thruster capacity is assumed to be equal to zero (Fig. 1b). The second one introduces spoiled zones, where the capacity of the thruster is reduced to a fraction of its maximum value (Fig. 1b).

Flushing another working thruster in the DP causes a drop in the efficiency of both the thruster that is doing the flushing and the one being flushed. The former is associated with the interaction of the propeller (thruster) jet with the other thruster (obstacle). The water jet hits the obstacle, disturbing the wake behind. The obstacle could also be a skeg or another non-working thruster. The latter is due to the drastically changed inflow to the flushed thruster and its propeller. The accelerated flow causes a drop in the propeller thrust as the angle of the inflow to the propeller blades increases, which in turn causes a change in the operational point of the propeller on the propeller characteristics curves. This phenomenon is complex to take into account as clearly defined losses. Therefore, the forbidden zone is applied to completely avoid the interaction.

An example of handling constraints for the azimuth thruster is shown in Fig. 1b. The approach is to divide the thrust constraint region into a set of convex safe zones (labelled and then into linearly approximated polygons. From these considerations, the zone boundary and saturation inequalities arise.

Zones Boundary Inequality Constraint. Following Assumption 4, the boundary conditions are formulated as linear inequalities [6]:

$$\begin{aligned} T_{\text{x}\,i} \sin\beta_{\text{start}\,z_i} - T_{\text{y}\,i} \cos\beta_{\text{start}\,z_i} &\leq 0 \\ -T_{\text{x}\,i} \sin\beta_{\text{end}\,z_i} + T_{\text{y}\,i} \cos\beta_{\text{end}\,z_i} &\leq 0 \end{aligned} \quad (3)$$

where $\beta_{\text{start}\,z_i}$, $\beta_{\text{end}\,z_i}$ denote the angles at which the zth zone of the ith thruster starts and ends, respectively

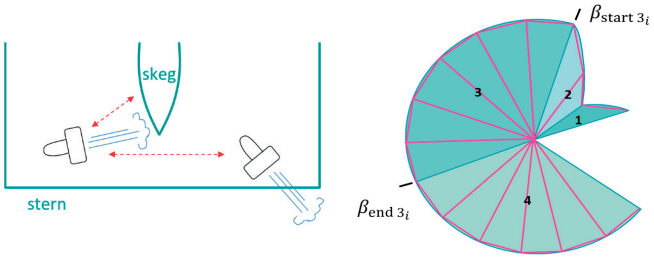

(a) Thruster flushing skeg and another working thruster *(b) th thruster capacity (background) and convex safe zones*

Fig. 1. Forbidden, spoiled zones and safe zones of azimuth thruster

Saturation Inequality Constraints. Two mechanisms of polygon description are provided, depending on the zone shape. First is for the circle-shaped zone (e.g., Fig. 1b, zones 3, 4) [6]:

$$T_{\text{x}\,i} \cos\left(\varphi_j\right)_i + T_{\text{y}\,i} \sin\left(\varphi_j\right)_i \leq r_i \quad (4)$$

where r_i is the maximum effective thrust of the ith thruster and φ_j refers to the ith middle angle of the polygon. An

illustration of the resulting polygon is provided in Fig. 2a. Second is for the spoiled zones (e.g., Fig. 1b, zones 1,2) [6]:

$$T_{\mathrm{x}\,i}(y_{k+1}-y_k)+T_{\mathrm{y}\,i}\,(x_{k+1}-x_k)\le x_k y_{k+1}-x_{k+1}y_k \quad (5)$$

where x_k, y_k are the coordinates of the first point, while x_{k+1}, y_{k+1} are the coordinates of the subsequent point. An illustration is provided in Fig. 2b.

Taking m_{z_i} as the total number of polygons within the ith zone of the ith thruster to describe a single zone, a system of m_{z_i} linear inequalities is needed. In practice, the number of polygons into which the zone is divided determines the accuracy of the method and shall be chosen individually for each case [6].

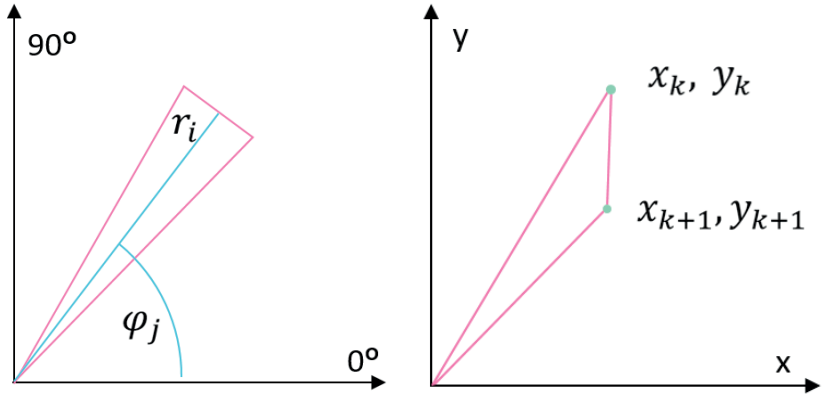

(a) Saturation – circle-shaped zone *(b) Saturation - spoiled zone*

Fig. 2. Inequality constraints - azimuth thruster

Propeller with rudder

In the presented approach, the rudder angle is not a decision variable as it cannot be approximated to a quadratic relation to power. Instead, a thrust region of the propeller representing all possible rudder angles is introduced, and the thrust–power quadratic relation can be maintained. Considering the boundaries of the maximum angle of the rudder on both sides, a convex thrust region can be defined by application of the methodology given in Eq. (3) and Eq. (5). Two convex thrust regions of the propeller with rudder are depicted in Fig. 3 with the linearisation mechanism applied. Region I is the reverse mode of the propeller and region II is the forward mode, accounting for rudder angle settings from -30° to 30°. After the optimisation, the rudder angle can be found by application of the approximately linear relation between the thrust angle and rudder angle. Another constraint needs to be defined for the reverse mode of the propeller, as described below. This creates two separate convex zones of the propeller with the rudder and these are to be taken into the optimisation process separately.

$$-T_{\max i}\le T_{\mathrm{x}\,i}\le 0\ \cap\ T_{\mathrm{y}\,i}=0 \quad (6)$$

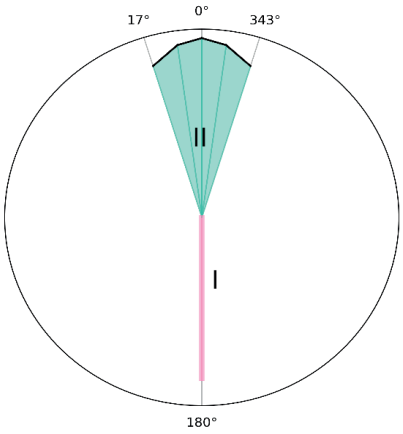

Fig .3. Propeller with rudder convex thrust regions

System of equations

The number of sub-problems to solve separately with the QP solver will be equal to the combination of all the convex zones of all the thrusters. In the case of the azimuth thruster, it could be up to 5 to 6 zones per thruster, and for the propeller with rudder it is 2. Matrices of constraints are built to define a system of equations. For the azimuth thruster for each thruster, they consist of two equations defined in Eq. (3) together with the set of equations defined in Eq. (4) or Eq. (5) in the case of spoiled zones. For the propeller with rudder, the system of equations is Eq. (3) with the set of equations defined in Eq. (5) and, in the case of a reverse mode, the set of equations corresponding to Eq. (6) is applied.

OBJECTIVE FUNCTION

By virtue of Assumption 3, the TA is assessed by considering an objective function (P_{total}) that yields a quadratic approximation of the total power consumption as a function of the generated forces:

$$P_{\mathrm{total}}(\boldsymbol{u}) \stackrel{\mathrm{def}}{=} \boldsymbol{u}^T\boldsymbol{W}\boldsymbol{u} \quad (7)$$

where $\boldsymbol{W} \stackrel{\mathrm{def}}{=} diag(w_1, w_1, w_2, w_2, \ldots, w_{\mathrm{N}}, w_{\mathrm{N}})$ is a diagonal matrix of weight coefficients w_i, $\forall_i$, corresponding to each mounted thruster. The weight coefficients are determined according to [1] with the exception that the maximum thrust loss in the case of spoiled zones is also considered.

OPTIMISATION TASK DECOMPOSITION

Due to the nature of the constraints, e.g., free variables, the problem of thrust allocation is decomposed into several sub-problems to be solved independently using a QP approach. The best amongst all the solutions found is selected by comparison. Considering all possible combinations of the thruster's convex zones and rudder angle cases, the number of optimisation tasks is given by $L = \prod_{i=1}^{N} Z_i$, where Z_i represents the total number of zones of the ith thruster. In the case of the azimuth thruster, the possible interactions impose decomposition of the optimisation task into Z_i convex sub-problems as in Eq. (3). Subsequently, in the case of the propeller with the rudder, Z_i denotes the total number of sub-problems, which is two (forward and reverse mode). The QP-based thrust allocation task for the ith sub-problem yields:

$$\begin{aligned} \mathrm{QP}_l: \quad & \boldsymbol{u}_l := \arg\min_{\boldsymbol{u}} P_{\mathrm{total}}(\boldsymbol{u}) \\ & s.t. \quad \boldsymbol{A}_l \boldsymbol{u} = \boldsymbol{b} \\ & \quad\;\; \boldsymbol{G}_l \boldsymbol{u} \leq \boldsymbol{h}_l \end{aligned} \tag{8}$$

where $\boldsymbol{A}_l$ and $\boldsymbol{G}_l$ are the equality and inequality constraints matrices; $\boldsymbol{b}$ denotes a vector encompassing forces and moments; $\boldsymbol{h}_l$ represents the thrust saturation and limiting operation angle. The internal structure of the vectors and matrices results directly from Eq. (3) – (6).

The best thrust allocation ($\boldsymbol{u}^*$) is found by comparison between the L results as stated below:The best thrust allocation is found by comparison between the results as stated below:

$$\begin{aligned} & \boldsymbol{u}^* := \arg\min_{\boldsymbol{u}_l} \{P_{\mathrm{total}}(\boldsymbol{u}_l)\} \\ & s.t. \;\; \boldsymbol{u}_l \leftarrow \mathrm{QP}_l \;\wedge l \in \overline{1, L} \end{aligned} \tag{9}$$

where $P_{\mathrm{total}}(\boldsymbol{u}_l)$ is the total power related to the solution of Eq. (8).

DP CAPABILITY ASSESSMENT

Finally, the ship's DP capability is assessed in the following manner. The problem Eq. (8) – (9) is solved for discrete values of angle (from 0° to 360°) and increasing levels of the impact of environmental forces. The exact number of combinations varies from ship to ship, to cover the whole considered domain of interest. Consequently, a population of results is obtained for each environmental angle considered. In each case, the result is obtained by applying the minimum operator. The DP capability results are typically presented in graphic form, as a polar plot, where each circle in the plot represents a DP number corresponding to a specific weather condition [1].

PROGRAM FLOWCHART

The DP Capability plot program has been coded using Python 3.8 programming language extended with the *qpsolvers* library, delivering the *quadprog* solver used to handle the optimisation problem of Eq. (9) [28]. The flowchart illustrating the program data flow is presented in Fig. 4. Fig. 4a presents the main part of the program routine, while the sub-process directly invoking the optimisation task (Eq. (8)) is illustrated in Fig. 4b. The logic of the program is as follows. First, the program reads the user-generated inputs, namely the basic hull and thruster data (Fig. 4a). In the same step, the propeller coefficients /or azimuth thruster's losses are calculated based on the DNV standard, while the loop of environmental angles (γ) and DP numbers ($\mathrm{k_{DP}} \in \overline{1, \mathrm{n_{DP}}}$) is initiated.

Second, the environmental force calculation combines the basic hull data and environmental (wind, current and wave) coefficients. The maximum ventilation losses and maximum effective thrust for each thruster are calculated. Third, the DP Capability Assessment sub-process is called. Within the sub-process (Fig. 4b), all the combinations of linear matrices $\boldsymbol{G}_l$,$\boldsymbol{h}_l$, $\boldsymbol{A}_l$, $\boldsymbol{b}$ and $\boldsymbol{W}_l$, for $l = 1 : L$ are calculated. These define all (L) possible combinations of the convex sets comprising the constraints. The process loops through these combinations, solving each time the problem defined by Eq. (8). The DP Capability Assessment sub-process ends by finding vector u^*, which corresponds to the minimal power consumption as defined by Eq. (9). At this point, the control flow is returned to the main routine and the program continues until the environmental angle and DP number conditions are satisfied. Fourth and last, the solution – DP Capability plot data – is saved and plots are generated. In the case of a loss of one of the thrusters, one must simply consider the only remaining thruster, noting that, in the case of the azimuth thruster, a spoiled zone due to flushing a dead thruster needs to be considered, as given in Eq. (5).

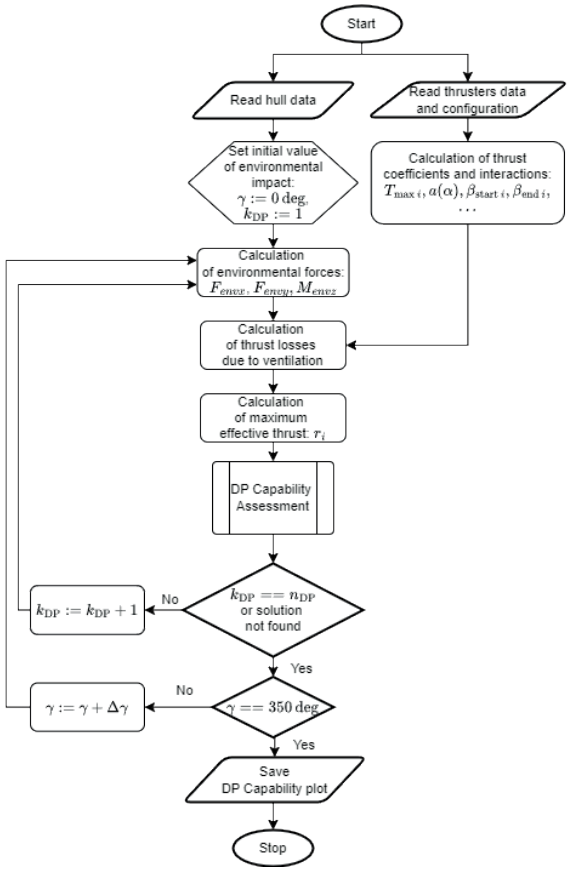

(a) DP Main routine

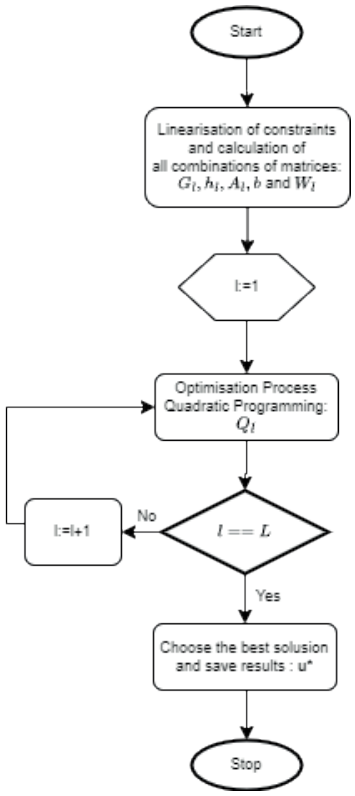

(b) DP Capability Assessment sub-process

Fig. 4. Flowchart of DP capability plot program

RESULTS

To illustrate the proposed approach, a case study was used to evaluate the DP capability of a rescue ship with an overall length of 96 m. The required data for the experiment regarding the ship's geometry are included in Tab. 1. The ship under analysis is equipped with five propellers (see Table 2). These include two azimuth thrusters at the stern, one azimuth thruster with a nozzle at the bow, and two tunnel thrusters at the bow. The discussed distribution of the propulsion system components is illustrated in Fig. 5a.

Tab. 1. General ship data

Symbol	Value	Unit	Description[1]
L_{pp}	86.6	*m*	Length between perpendiculars
B	18.8	*m*	Maximum breadth at waterline
T	5.0	*m*	Summer load line draft
L_{os}	95.85	*m*	Longitudinal distance between the foremost and aftmost point under water
X_{os}	-0.13	*m*	Longitudinal position of $L_{os}/2$
Bow_{angle}	27.4	°	Half bow angle of entrance
$A_{F,\,wind}$	392.0	m^2	Frontal projected wind area
$A_{L,\,wind}$	1203.0	m^2	Longitudinal projected wind area
$X_{L,\,wind}$	6.014	*m*	Longitudinal position of the area centre of $A_{L,\,wind}$
$A_{L,\,current}$	441.0	m^2	Longitudinal projected submerged current area
$X_{L,\,current}$	4.717	*m*	Longitudinal position of the area centre of $A_{L,\,current}$
x_{skeg}	-37.8	*m*	*x* position of the skeg aft edge
y_{skeg}	0	*m*	*y* position of the skeg aft edge

[1] Full definition of variables with the coordinate system is available in DNV standard [1].

Tab. 2. Thrusters main data

Description	Unit	Thruster 1	Thruster 2	Thruster 3	Thruster 4	Thruster 5
Thruster type	–	Azimuth thruster without nozzle / Shaft line with open FPP propeller	Azimuth thruster without nozzle / Shaft line with open FPP propeller	Azimuth thruster with nozzle	Tunnel thruster	Tunnel thruster
Rudder type	–	Not applicable / NACA	Not applicable / NACA	Not applicable	Not applicable	Not applicable
x	m	-41.076	-41.076	34.12	37.12	40.72
y	m	4.690	-4.690	0	0	0
x	m	1.540	1.540	-1.100	2.000	2.000
Propeller diameter, D	m	3.100	3.100	1.650	1.740	1.740
Engine brake power, P_{brake}	Kw	1325	1325	880	900	900
Rudder surface A_r	m^2	Not applicable / 6.000	Not applicable / 6.000	Not applicable	Not applicable	Not applicable

This section reports the results of the DP capability assessment obtained based on the approach described in the Methodology section. A tool developed using the Python programming language has been used for this purpose. It is important to note that the tool is in line with the DNV standard [1] Level 1, in which a so-called DP number is assigned to specific environmental conditions (wind, waves and currents). To improve legibility, firstly, an elementary example for two arbitrary angles is presented in the Optimal thrust allocation sub-section. Secondly, the evaluation of DP capabilities is discussed. Thirdly, the results obtained are compared with those obtained using the DNV on-line tool[2].

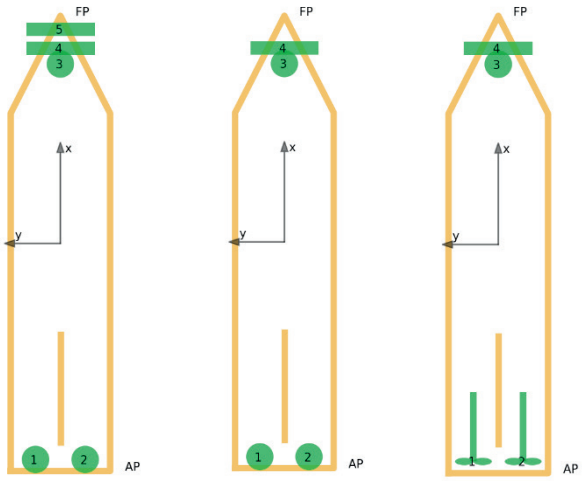

(a) Main thrusters – 5 azimuth thrusters

(b) Main thrusters – 4 azimuth thrusters

(c) Main thrusters – propeller with rudder – 4 thrusters

Fig. 5. Thrusters layout for analysed vessel

[2] The free version of the application is limited to analysis of a maximum four thrusters and does not share detailed results, just the DP capability plot.

The results analysed in this section include three cases. A comparative layout of the three cases is shown in Fig. 5. The first case (no. 1) includes all five thrusters presented in Table 3 with the layout depicted in Fig. 5a. In Fig. 6 and Fig. 7, the results of the DP capability evaluation for this case are presented. The second case (no. 2) considers the layout depicted in Fig. 5b and includes only the azimuthal thrusters in the analysis. The third case (no. 3), with the layout depicted in Fig. 5c, considers the azimuth, tunnel and rudder propellers as the main thrusters. In order to compare the results obtained by the presented method with those obtained from the free online application provided by DNV, the bow thruster was excluded from the analysis (in cases no. 2 and 3). This is due to the fact that the version of the DNV application provided allows analysis of ships with only up to four propellers. In addition, the efficiency of the propulsion system with azimuthal thrusters was compared with the system where the propulsion system consists of thrusters with rudders. The results of the DP capability assessment for the second and third cases are compared in Fig. 8 with the DNV online application.

OPTIMAL THRUST ALLOCATION

The direct result of the calculation is the thrust allocation (thrust components in the and direction for all thrusters). An example of optimal thrust allocation for two distinct angles, namely 10° and 90°, calculated under environmental conditions set to DP number 6 [1], is presented in Fig. 6 for case no. 1 and the TA results are listed in Table 3.

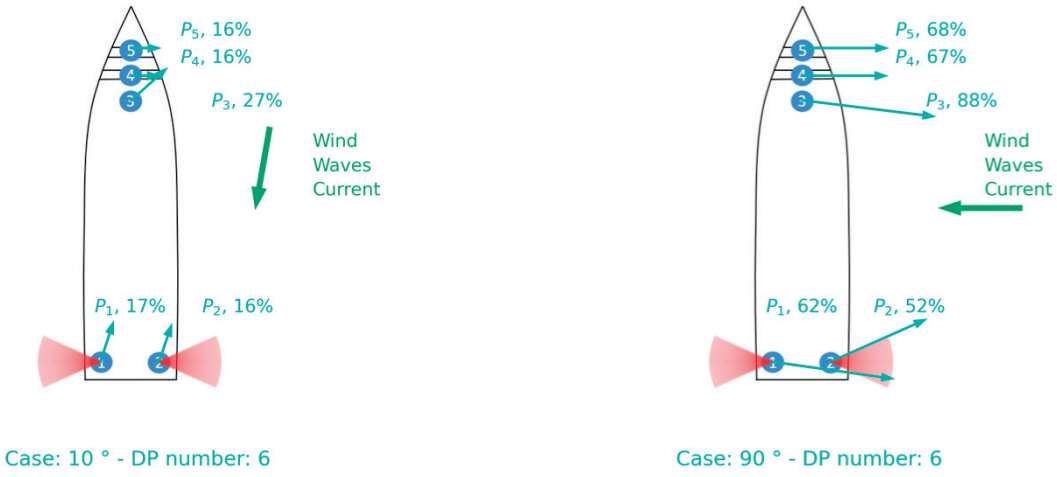

(a) Environmental angle 10° *(b) Environmental angle 90°*

Fig. 6. Optimal thrust allocation

Tab. 3. Results of optimal thrust allocation as effective thrust vector values

Effective thrust [kN]										
Thruster	1		2		3		4		5	
Force component	$T_{x,1}$	$T_{y,1}$	$T_{x,2}$	$T_{y,2}$	$T_{x,3}$	$T_{y,3}$	$T_{x,4}$	$T_{y,4}$	$T_{x,5}$	$T_{y,5}$
Case 10 °	28	-9.5	25.6	-9.5	23.7	-25.6	0	-15.9	0	-16.4
Case 90 °	-15.4	-108.6	37.4	-84.1	-14.8	-113	0	-68.2	0	-68.6

The location of the thrusters is indicated with blue numbered dots. The red areas near the rear thrusters indicate the forbidden zones. The result of the thrust allocation is indicated by the turquoise arrows attached to the thrusters. For legibility of the result, the percentage of maximum thrust is displayed to clearly characterise the magnitude of the thrust vectors

As a result of the analysis, one can clearly identify that the environmental impact from the 90° direction causes higher engagement of the thrusters. In both cases, it can be observed that the most utilised thruster is the bow azimuth thruster. At the 10° direction, the thrust utilisation is significantly reduced. This directly relates to the ship's geometry, both under and above the water level, and the exerted environmental forces and moments that depend on it.

DP CAPABILITY ASSESSMENT

The DP capability plot is a result of a true/false solution of the QP solver. In the case of true, the solution is found, the thrust allocation is performed allowing for the power consumption to be determined, and the ship is capable of keeping its position. In the case of false, the ship cannot maintain its position. The solver loops through the environmental angles and conditions (in total up to 396 cases) to return the DP capability plot.

Fig. 6 presents the results of the DP capability assessment (case no. 1), showcasing both the DP capability and the power envelope for a selected scenario (DP number 3). Three DP operation modes have been investigated. First is "intact", where all the thrusters are considered operational. Second is a single failure, where one of the thrusters failed, and two scenarios were explored, one considering the failure of thruster 2 and second of thruster 3 (location given in Fig. 5). Third is the worst-case scenario which, in this case, is loss of the switchboard. In both failure scenarios and the worst-case scenario, the DP capability is significantly reduced. The DP system is more effective at DP number 3 in the intact case than in other cases, especially the worst-case scenario, which is the most power-consuming.

The results from the developed tool were compared to those obtained using the on-line application by DNV (Fig. 7). It was found that, in the case of using azimuth thrusters as the main propulsion (case no. 2), the results obtained from both tools are the same (Fig. 7a). However, the results obtained considering propellers with the rudder as the main thruster (case no. 3) vary significantly (Fig. 7b). In general, the methodology presented in this work shows a more pessimistic outcome in comparison to the DNV web application. Further investigation of the discrepancies is required to gain a better understanding of the matter.

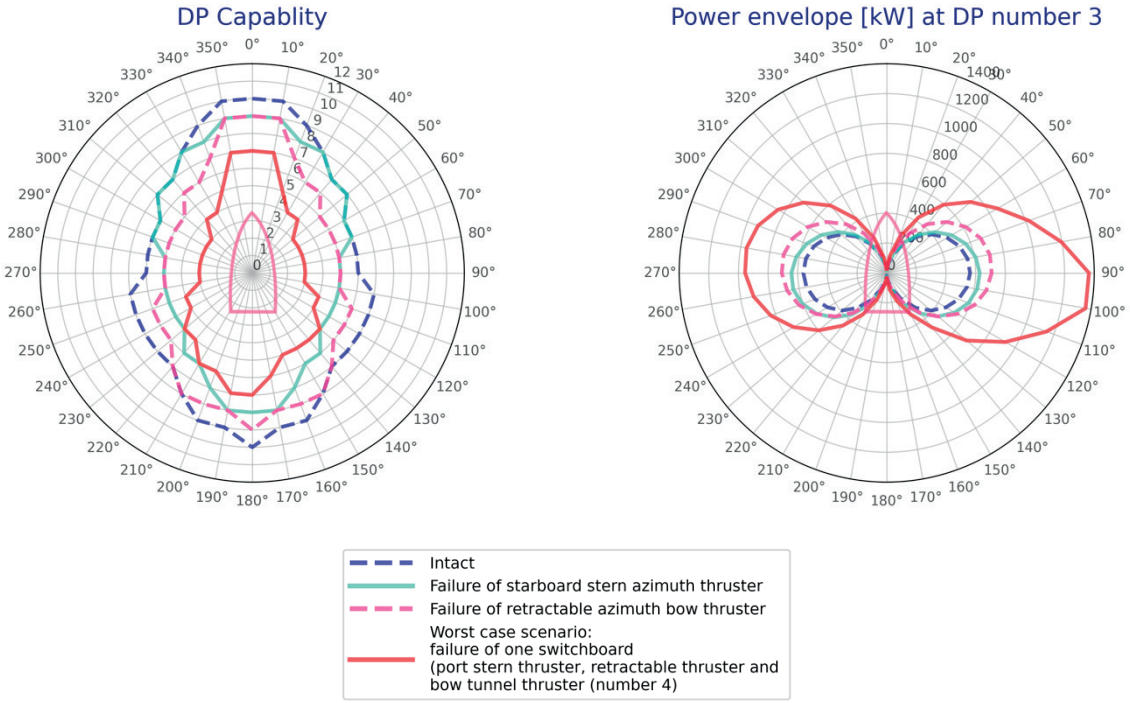

(a) DP capability plot *(b) Power consumption polar plot*

Fig. 7. Comparison of selected cases

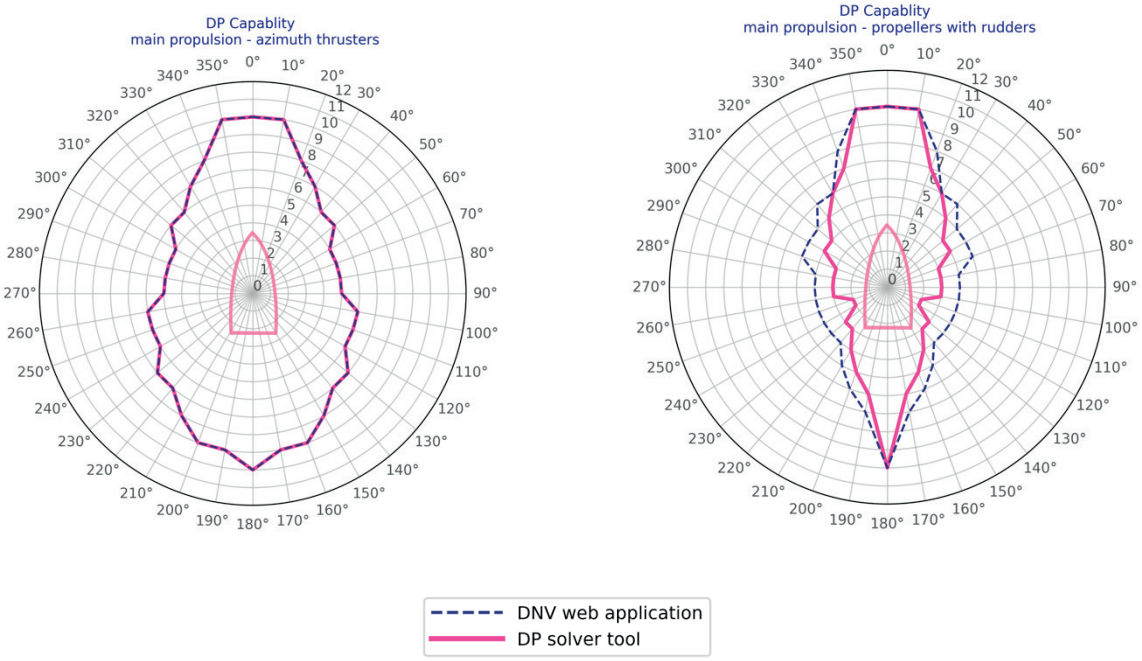

(a) 4 thrusters - two aft propulsors: azimuth thrusters *(b) 4 thrusters - two aft propulsors: propellers with rudders*

Fig. 8. Comparison of DP capability plots

CONCLUSIONS

The recently increasing need for DP assessment tools, both fast rough calculations as well as time-domain simulations for the early stage of the design, was the motivation for the study. The quadratic programming method used in optimal thrust allocation provided relevant results when applied to DNV rules (DNV-ST-0111 standard). This was evident while concerned with handling the influences between the thrusters and the skeg. The guidelines and rules provided by the DNV classification society are very popular and are often applied in the ship design phase in typical design offices around the world. Thus, the presented method could be effectively used by designers for rough initial calculations without a need for investment in expensive software.

The presented method is handy while making comparisons between different designs and especially when selecting the size and power of the thrusters at the early design stage. However, it should be treated only as the initial evaluation before contracting for making an offer. This is due to the lack of sufficient validation data for the TA evaluation. Moreover, the DNV guidelines are based on the empirical formulas and therefore the results should be treated as an approximation of the DP performance. The DP capability assessment of a ship equipped with propellers with rudders reveals some discrepancies when compared with the results obtained using DNV's online application. Further research in this area, including validation with a broader group of ships of different types, is likely to yield a better insight into this problem.

It is important to mention that, due to the adopted methodology (thrust forces being the decision variables), it was not possible to apply the ventilation losses according to DNV-DT-0111 correctly. Among other factors, the losses depend on the propeller loading (thrust), but the thrust is the result of the optimisation, therefore it was not possible to take it into account when preparing the input to the QP solver. Losses are not dependent on thrust loading for sufficiently deep draughts or lower sea states. This varies from ship to ship. The maximum losses (for the maximum loading) are adopted instead, which can lead to an extremely pessimistic result in the case of a vessel with very low draught relative to the propeller's vertical position.

An important element of future research will be the evaluation of the accuracy of the method based on time-domain simulation and model tests. Verification of the simulation is planned based on experiments on the dedicated test stand of the Maritime Advanced Research Centre, using the physical model of the ship, equipped with a DP system.

REFERENCES

1. DNV, DNV-ST-0111, Assessment of station keeping capability of dynamic positioning vessels, DNV, 2021.
2. M. Tomera, "Dynamic positioning system for a ship on harbour manoeuvring with different observers. Experimental Results," Polish Maritime Research, 2014.
3. M. Tomera, "Dynamic positioning system design for "Blue Lady". Simulation tests," Polish Maritime Research, 2012.
4. T. Fossen, Handbook of Marine Craft Hydrodynamics and Motion Control, 1st ed. New York: John Wiley, 2011.
5. A. Sørensen, „Marine Control Systems. Propulsion and Motion Control of Ships and Ocean Structures," Lecture Notes, Department of Marine Technology. Norwegian University of Science and Technology, 2013.
6. C. de Wit, „Optimal thrust allocation methods for dynamic positioning of ships," M.Sc. thesis, Delft University of Technology, 2009.
7. S. Luke, "Essentials of Metaheuristics," in Lecture Notes, Second Edition , 2016.
8. J. Ming and Y. Bowen, „The optimal thrust allocation based on QPSO algorithm for dynamic positioning vessels," Tianjin, China, 2014, doi: 10.1109/ICMA.2014.6885898.
9. X. Yang, "Optimization and metaheuristic algorithms in engineering," in Metaheuristics in Water, Geotechnical and Transport Engineering, Elsevier, 2013, pp. 1-23.
10. G. Ding, P. Gao, X. Zhang, and Y. Wang, "Thrust allocation of dynamic positioning based on improved differential evolution algorithm," in Proc. 39th Chinese Control Conference, Shenyang, China, doi: 10.23919/CCC50068.2020.9188704, 2020.
11. R. Storn and K. Price, "Differential evolution - A simple and efficient adaptive scheme for global optimization over continuous spaces," Journal of Global Optimization, vol. 23, no. 1, 1995.
12. D. Goldberg, Genetic Algorithms in Search, Optimization & Machine Learning. Addison-Wesley, 1989.
13. T. Baetz-Beielstein, „Overview: Evolutionary Algorithms," Ph.D. project, Cologne University of Applied Sciences, 2014.
14. M. Kochenderfer and T. Wheeler, Algorithms for Optimisation. MIT Press, 2019.
15. E. Baeyens, A. Herreros, and J. Perán, "A direct search algorithm for global optioptimization," Algorithms, vol. 9, no. 2, p. 40, 2016, https://doi.org/10.3390/a9020040.
16. K. Deb, A. Pratap, S. Agarwal, and T. Meyarivan, "A fast and elitist multiobjective genetic algorithm: NSGA-II," IEEE Transactions on Evolutionary Computation, vol. 6, no. 2, pp. 182-197, 2002, doi: 1109/4235.996017.

17. D. Gao, X. Wang, T. Wang, Y. Wang, and X. Xu, "Optimal thrust allocation strategy of electric propulsion ship based on improved non-dominated sorting genetic algorithm II," IEEE Access, vol. 7, no. 1, pp.135247-135255, 2019, doi: 10.1109/ACCESS.2019.2942170, 2019.

18. F. Mauro and R. Nabergoj, "Advantages and disadvantages of thruster allocation procedures in preliminary dynamic positioning predictions," Ocean Eng., vol. 123, pp. 96-102, 2016, https://doi.org/10.1016/j.oceaneng.2016.06.045.

19. O. Harkegard, "Dynamic control allocation using constrained quadratic programming," J. Guid. Contr. Dynam., vol. 27, no. 6, pp. 1028–1034, 2004, https://doi.org/10.2514/1.11607.

20. Y. Luo, A. Serrani, S. Yurkovich, D. B. Doman, and M. W. Oppenheimer, "Model predictive dynamic control allocation with actuator dynamics," in IEEE Proc. 2004 American Control Conference, pp. 1695–1700, 2004, doi: 10.23919/ACC.2004.1386823.

21. A. Witkowska and R. Śmierzchalski, "Adaptive backstepping tracking control for an over-actuated DP marine vessel with inertia uncertainties," Int. J. Appl. Math. Comput. Sci., vol. 28, no. 4, pp. 679–693, 2018, doi: 10.2478/amcs-2018-0052.

22. J. Tjønnås and T. Johansen, "Adaptive control allocation," Automatica, vol. 44, pp. 2754-2766, 2008, https://doi.org/10.1016/j.automatica.2008.03.031.

23. M. Valčič, „Optimization of thruster allocation for dynamically positioned marine vessels," Doctoral thesis, University of Rijeka, 2020.

24. E. Ruth, „Propulsion control and thrust allocation on marine vessels," Doctoral thesis, Norwegian University of Science and Technology, 2008.

25. L. Wang, J. Yang, and S. Xu, "Dynamic positioning capability analysis for marine vessels based on a DPCap polar plot program," China Ocean Eng., vol. 32, no. 1, pp. 90-98, 2018, doi: 10.1007/s13344-018-0010-4.

26. P. Zalewski, "Constraints in allocation of thrusters in a DP simulator," Sci. J. Mar.Univ. Szczecin, vol. 52, no. 124, pp. 45-50, 2017, doi: 10.17402/244.

27. P. Zalewski, "Convex optimization of thrust allocation in a dynamic positioning system," Sci. J. Mar.Univ. Szczecin, vol. 48, no. 120, pp. 58-62, 2016, doi: 10.17402/176.

28. D. Goldfarb and A. Idnani, "A numerically stable dual method for solving strictly convex quadratic programs," Mathematical Programming, vol. 27, pp. 1-33, 1983.